

Rotational properties of dipolar Bose-Einstein condensates in double-well potential

Cite as: AIP Conference Proceedings **2265**, 030019 (2020); <https://doi.org/10.1063/5.0017151>
Published Online: 05 November 2020

Thangarasu Sriraman, Ramavarmaraja Kishor Kumar, Rajamanickam Ravisankar, and Paulsamy Muruganandam



View Online



Export Citation

ARTICLES YOU MAY BE INTERESTED IN

[On the ground state phases in spin-orbit coupled Bose-Einstein condensates with weak repulsive interactions](#)

AIP Conference Proceedings **2265**, 030022 (2020); <https://doi.org/10.1063/5.0017155>

[Piezoelectricity and excellent thermal stability in \$W^{6+}\$ modified \$SrBi_4Ti_4O_{15}\$ ceramics](#)

AIP Conference Proceedings **2265**, 030018 (2020); <https://doi.org/10.1063/5.0017189>

[Arrest of growth of Ag nanoparticles in polymer matrix: A small-angle x-ray scattering study](#)

AIP Conference Proceedings **2265**, 030027 (2020); <https://doi.org/10.1063/5.0017088>

Meet the Next Generation
of Quantum Analyzers

And Join the Launch
Event on November 17th



Register now



Zurich
Instruments

Rotational Properties of Dipolar Bose-Einstein Condensates in Double-well Potential

Thangarasu Sriraman¹, Ramavarmaraja Kishor Kumar², Rajamanickam Ravisankar¹ and Paulsamy Muruganandam^{1, a)}

¹*Department of Physics, Bharathidasan University, Tiruchirappalli 620 024, TN, India*

²*Instituto de Física, Universidade de São Paulo, 05508-090 São Paulo, Brazil*

a) Corresponding author: anand@bdu.ac.in

Abstract. We investigate the impact of interplay between the contact interaction and the dipole-dipole interaction on the rotational properties of dipolar Bose-Einstein condensate, rotating in an axially confined double-well potential. The dynamics is governed by a quasi-two-dimensional Gross-Pitaevskii equation with phenomenological dissipation and non-local dipole-dipole interaction integral. In the present study, we consider using three different dipolar atoms namely ^{52}Cr , ^{168}Er and ^{164}Dy with increasing order of dipole-dipole interaction strength respectively. From our numerical simulation, we see, at the critical frequency, the vortex core starts to emerge from the peripheries of the BEC. Further, we observe that the critical frequency of vortex nucleation decreases with an increase of dipole-dipole interaction strength and contact interaction strength and these interactions also enhance the number of vortices. We also find that the increase in average angular momentum per atom with rotational frequency suddenly shifts from linear to non-linear progression after attaining the critical rotational frequency. From the results obtained in the present study, it is quite clear that dipole-dipole interaction and contact interaction compliments with each other, has a considerable influence on the rotational properties of dipolar BECs.

I. INTRODUCTION

Bose-Einstein condensates (BECs) of atoms with large magnetic dipole moments, the dipolar BECs or dipolar condensates, have been experimentally realized in a gas of chromium (^{52}Cr) atoms, followed by dysprosium (^{164}Dy) and erbium (^{168}Er)¹. In these dipolar condensates, the inter-atomic interactions are mainly dominated by a short range isotropic s-wave contact interaction (CI) and a long range anisotropic dipole-dipole interaction (DDI). By spinning the quantization axis of the atomic dipoles, tuning of the DDI is possible² along with the Feshbach tuning of the CI. The rotational properties of dipolar Bose gases have also been studied theoretically in mean-field regime^{3, 4}. The studies display that as quite similar to that of ground state properties, the rotational property is also strongly influenced by decisive factors, such as harmonic trap aspect ratio, DDI strength, CI strength and relative strengths between DDI and CI^{4, 5}. In the literature, several techniques are available regarding the nucleation of vortices in trapped BECs. It is recognized that a BEC in a rotating harmonic trap, there is a critical rotation frequency beyond which, vortex starts to exist⁶. With the increasing of rotation frequency, more and more vortices appear. Recently, Linghua Wen et.al⁷ conducted a theoretical investigation on the Feynman rule for the number of vortices in a rotating double-well (DW) potential. Even though the vortices can appear in other external potential, the central barrier in the DW potential assists to visualize the conversion of hidden vortices to visible core. In this sense, the DW potential provides a unique ground for testing Feynman rule in rotating BECs. It would be interesting to study the vortex state of dipolar BEC in a DW potential along with DDI and CI. In the present work, we focus on the influence of DDI and CI on the rotational properties of dipolar BEC. Through the numerical simulation of dipolar BEC, rotating in DW potential, we calculate the number of vortices (N_v) and the average angular momentum per

atom ($\langle L_z \rangle$) for pure dipolar BECs and dipolar BECs in the presence of repulsive CI, as a function of rotational frequency (Ω). This paper is organized as follows: In Sec. II, we present the effective 2D Gross-Pitaevskii equation to study a dipolar BEC in a rotating DW potential as well as the numerical discretization scheme used in the simulation. In Sec. III, we discuss the various results obtained. Finally, in Sec. IV, we also present a brief summary and conclusion.

II. MEAN FIELD MODEL

Considering pancake shaped BEC with strong axial confinement rotating in a DW potential, where the DW potential is described⁷ by,

$$V_{DW} = \frac{1}{2}(x^2 + \lambda^2 y^2) + V_0 e^{-x^2/2\sigma^2} \quad (1)$$

where, $\lambda = \omega_y/\omega_x$ is the trap anisotropy parameter and ω_x, ω_y are the corresponding angular frequency in the x and y direction of the harmonic trap, V_0, σ are the respective height and width of the central barrier of DW.

Using mean field Gross-Pitaevskii (GP) equation^{6, 8}, vortex dynamics of BEC can be studied. The dynamics of dipolar BEC consisting of N atoms, each of mass m at ultracold temperature, having strong axial confinement is described by the following effective 2D GP equation^{9, 10, 11},

$$(i - \gamma) \frac{\partial \phi_{2D}(\boldsymbol{\rho}, t)}{\partial t} = \left[-\frac{\nabla_{\boldsymbol{\rho}}^2}{2} + V_{2D} - \Omega L_z + \frac{4\pi a N}{\sqrt{2\pi} d_z} |\phi_{2D}(\boldsymbol{\rho}, t)|^2 \right. \\ \left. + \frac{4\pi a_{dd} N}{\sqrt{2\pi} d_z} \int \frac{d^2 k_{\rho}}{(2\pi)^2} e^{-i\mathbf{k}_{\rho} \cdot \boldsymbol{\rho}} \tilde{n}(\mathbf{k}_{\rho}) h_{2D}\left(\frac{k_{\rho} d_z}{\sqrt{2}}\right) \right] \phi_{2D}(\boldsymbol{\rho}, t) \quad (2)$$

In Eq. (2), γ is the phenomenological dissipation, $\phi_{2D}(\boldsymbol{\rho})$ is the 2D wavefunction with normalization $\int |\phi_{2D}(\boldsymbol{\rho}, t)|^2 d\boldsymbol{\rho} = 1$, V_{2D} is the effective 2D confining potential, in our case, it's the DW potential in Eq. (1), Ω is the external rotational frequency of the BEC acting through the z axis, $L_z = -i(x\partial_y - y\partial_x)$, which corresponds to the z component of the angular momentum, due to the rotation of the BEC, a is the atomic scattering length, $d_z = \sqrt{1/\omega_z}$, where, ω_z is the angular frequency of harmonic trap in the z direction, $a_{dd} = \mu_0 \bar{\mu}^2 m / 12\pi \hbar^2$, is the characteristic dipole length, $\bar{\mu}$ corresponds to the magnetic dipole moment of a single atom and μ_0 the permeability of free space. The experimental value for a_{dd} of ^{52}Cr , ^{168}Er and ^{164}Dy are $16a_0$, $66a_0$, and $130a_0$, respectively, where, a_0 is the Bohr radius. The $\tilde{n}(\mathbf{k}_{\rho})$ in Eq. (2) follows :

$$\tilde{n}(\mathbf{k}_{\rho}) = \int \exp(i\mathbf{k}_{\rho} \cdot \boldsymbol{\rho}) |\phi_{2D}(\boldsymbol{\rho})|^2 d\boldsymbol{\rho} \quad (3)$$

where, $\mathbf{k}_{\rho} \equiv (k_x, k_y)$, $h_{2D}(\xi) = 2 - 3\sqrt{\pi}\xi \exp \xi^2 \text{erfc}(\xi)$, and the dipolar term is written in Fourier space. In Eq. (2) length is measured in units of characteristic harmonic oscillator length, $l \equiv \sqrt{\hbar/m\omega_z}$, frequency in units of ω_z and energy in units of $\hbar\omega_z$. To study the rotational properties of dipolar BECs, we carry out a numerical simulation by solving Eq. (2) using split-step Crank-Nicolson based numerical scheme described in^{11, 13, 14}. In the present investigation, the value of phenomenological dissipation is set as $\gamma = 10^{-5}$, the number of atoms is fixed as $N = 2 \times 10^4$ and the DDI is altered by varying a_{dd} through the choice of three different dipolar atoms viz., ^{52}Cr , ^{168}Er and ^{164}Dy with increasing order of characteristic dipole length respectively. The simulation is performed with the $x \times y$ grid, set as 200×200 ; space step ($\Delta x = \Delta y$) and time step (Δt) are set as 0.2 and 0.004, respectively.

III. RESULTS AND DISCUSSION

i. Effect of DDI and CI on the Number of Vortices

In this section, we will discuss about the effect of CI and DDI on the number of vortices. Figure 1, displays the plot of numerically calculated number of vortices as a function of the rotational frequency Ω for various dipolar atomic BECs namely ^{52}Cr , ^{168}Er and ^{164}Dy .

Figure 1 (a), depicts the case of pure dipolar BEC ($a = 0a_0$) of the latter dipolar atoms, whereas Fig. 1 (b), is for the case of dipolar BECs with repulsive CI of positive atomic scattering lengths, $a = 40a_0$. We also investigate the cases of dipolar BECs in the presence of attractive CI, which seems to be very unstable, even in the absence of rotation. Hence, we neglect that case in the present study.

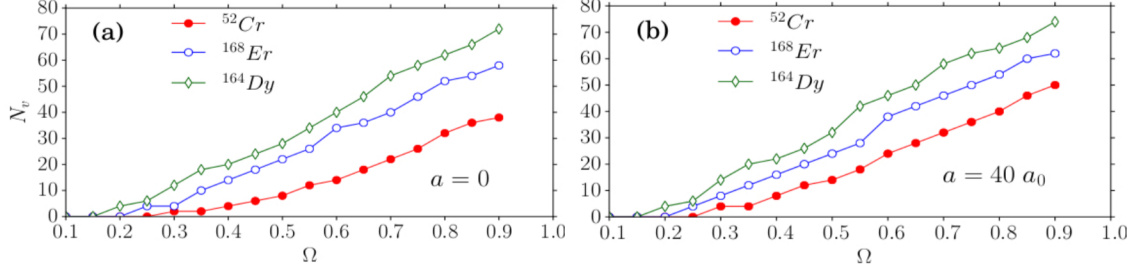


FIGURE 1. Plot of the numerically computed equilibrium number of vortices (N_v) as a function of the rotational frequency (Ω) of dipolar BECs ^{52}Cr , ^{168}Er and ^{164}Dy for few values of atomic scattering lengths (a) $a = 0a_0$ and (b) $a = 40a_0$.

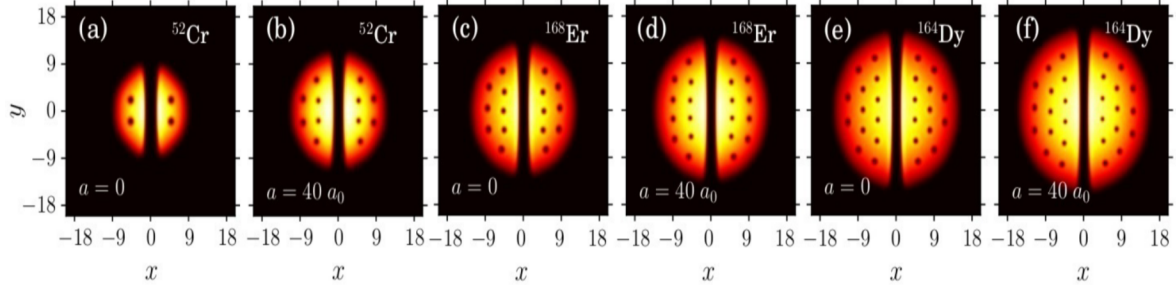


FIGURE 2. Contour plots of density distribution $|\phi_{2D}|^2$ showing steady state vortices in a rotating dipolar BEC with $\Omega = 0.4$, $N = 2 \times 10^4$, $\lambda = 1$. For ^{52}Cr , (a) $a = 0a_0$ and (b) $a = 40a_0$. For ^{168}Er , (c) $a = 0a_0$ and (d) $a = 40a_0$. For ^{164}Dy , (e) $a = 0a_0$ and (f) $a = 40a_0$.

In all the cases of dipolar BECs with and without CI, the number of vortices, is a monotonically increasing function of rotational frequency. Though, both CI and DDI interaction have a impact on the number of vortices, the role of CI on the number of vortices is relatively less, as compared to the DDI. From Fig. 2, it is evident that the number of vortices in BEC of ^{164}Dy has the highest value, followed by ^{168}Er and ^{52}Cr .

ii. Average Angular Momentum vs. Rotational Frequency

At a critical rotational frequency, vortices commence to emerge from the condensate in the regions of lower concentration of atoms and from there onwards the average angular momentum per atoms ($\langle L_z \rangle$) grows exponentially with the rotation frequency⁷. $\langle L_z \rangle$ is calculated by

$$\langle L_z \rangle = i \int \phi_{2D}^*(\mathbf{r}, t) (x\partial_y - y\partial_x) \phi_{2D}(\mathbf{r}, t) d\mathbf{r} \quad (4)$$

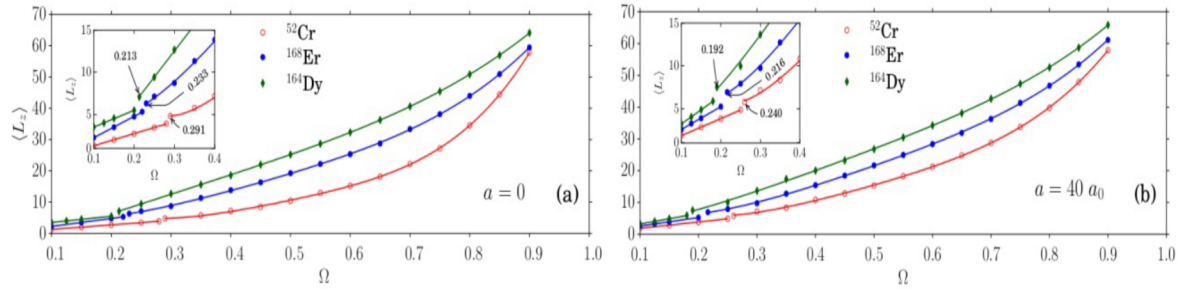


FIGURE 3. Plot of average angular momentum per atom ($\langle L_z \rangle$) as a function of the rotational frequency (Ω) of dipolar BECs of ^{52}Cr , ^{168}Er and ^{164}Dy for few values of atomic scattering lengths (a) $a = 0a_0$ and (b) $a = 40a_0$. The values marked on the data points in the insert correspond to the critical rotational frequency.

Pure dipolar BECs and dipolar BECs in the presence of CI, also shows a linear relation with rotation frequency below the critical rotational frequency. However, after attaining the critical rotational frequency, in contrast to the non-polar BEC, $\langle L_z \rangle$ of dipolar BECs, increases with Ω in a much slower rate. In Fig. 3, we plot $\langle L_z \rangle$ as a function of the rotational frequency (Ω), in which the numerical fit of the data points of $\langle L_z \rangle$, as a function of Ω from the point of critical rotation frequency (that is after discontinuity) confines to a quartic polynomial curve.

From Fig. 3, it is quite evident that the average angular momentum increases with increase of DDI. We can also observe from the panels (a) and (b) of Fig. 3, the separation between the curves among the dipolar atoms in each panel, is found to be decreasing with increase of atomic scattering length. In other words, the difference in angular momentum of BECs in different dipolar atoms decreases with increase of CI.

IV. SUMMARY AND CONCLUSION

From the present study, we obtain the results of different rotational properties of dipolar BECs in the presence of CI and DDI. Here, we employ the effective 2D GP equation with phenomenological dissipation for a dipolar BEC in DW potential. Further, we calculate numerically the number of vortices and the average angular momentum per atom for pure dipolar BECs and also for dipolar BECs in the presence of repulsive CI, as a function rotational frequency. The number of vortices and the average angular momentum are found to be monotonically increasing function of rotational frequency. We also compute the critical rotational frequency of vortex nucleation which seems to be decreasing with increase of DDI and CI. However, DDI has a relatively greater influence over CI in decreasing the critical rotational frequency. The dipolar BECs in the presence of repulsive CI is always found to be complement the DDI, in general, and these interactions possess a great impact on the rotational property.

V. REFERENCES

1. A. Griesmaier, J. Werner, S. Hensler, J. Stuhler, and T. Pfau, *Phys. Rev. Lett.* **94**, 160401 (2005).
2. S. Giovanazzi, A. Görlitz, and T. Pfau, *Phys. Rev. Lett.* **89**, 130401 (2002).
3. I. Coddington, P. Engels, V. Schweikhard, and E. A. Cornell, *Phys. Rev. Lett.* **91**, 100402 (2003).
4. M. Abad, M. Guilleumas, R. Mayol, M. Pi, and D. M. Jezek, *Phys. Rev. A* **81**, 043619 (2010).
5. R. K. Kumar, and P. Muruganandam, *J. Phys. B: At. Mol. Opt. Phys.* **45**, 215301 (2012).
6. A. L. Fetter, *Rev. Mod. Phys.* **81**, 647 (2009).
7. L. Wen, H. Xiong, and B. Wu, *Phys. Rev. A* **82**, 053627 (2010).
8. W. Bao, and H. Wang, *J. Comput. Phys.* **217**, 612 (2006).
9. P. Pedri, and L. Santos, *Phys. Rev. Lett.* **95**, 200404 (2005).
10. U. R. Fischer, *Phys. Rev. A* **73**, 031602(R) (2006).
11. P. Muruganandam, and S. K. Adhikari, *Laser Phys.* **22**, 813 (2012).
12. S. H. Youn, M. Lu, U. Ray, and B. L. Lev, *Phys. Rev. A* **82**, 043425 (2010).
13. P. Muruganandam, and S. K. Adhikari, *Comp. Phys. Commun.* **180**, 1888-1912 (2009).
14. R. K. Kumar, L. E. Young-S, D. Vudragović A. Balaž, P. Muruganandam, and S. K. Adhikari, *Comp. Phys. Commun.* **195**, 117-128 (2015).